frontiers | Frontiers in Materials

TYPE Original Research
PUBLISHED 18 December 2023
DOI 10.3389/fmats.2023.1332168

OPEN ACCESS

EDITED BY
Xiaolong Sun,
Guangdong University of Technology, China

REVIEWED BY
Zongwu Chen,
China University of Geosciences Wuhan, China
Ning Li,
Hohai University, China
Zhuangzhuang Liu,
Chang'an University, China

*CORRESPONDENCE
Peng Xiao,
pengxiao@yzu.edu.cn

RECEIVED 02 November 2023
ACCEPTED 27 November 2023
PUBLISHED 18 December 2023

CITATION
Li B, Zhang Y, Xiao P, Wang Y, Kang A and Zhang Y (2023), Comparative performance evaluation of basalt fiber–modified hot in-place (HIP) recycling asphalt mixtures: site mixture versus lab mixture.
Front. Mater. 10:1332168.
doi: 10.3389/fmats.2023.1332168

Comparative performance evaluation of basalt fiber–modified hot in-place (HIP) recycling asphalt mixtures: site mixture versus lab mixture

Bo Li[1,2], Yu Zhang[1], Peng Xiao[1,2]*, Yu Wang[1], Aihong Kang[1,2] and Yao Zhang[1,2]

[1]College of Civil Science and Engineering, Yangzhou University, Yangzhou, China, [2]Research Center for Basalt Fiber Composite Construction Materials, Yangzhou, China

The performance improvement of hot in-place recycling asphalt mixtures has been a hot topic recently due to the widespread application of HIP recycling technology. Based on the maintenance project of the provincial pavement G233 Baoying section, basalt fibers were introduced into HIP recycling mixtures. The effect of basalt fiber on the comprehensive performance of recycled mixtures was investigated using high temperature stability tests, cracking resistance tests, water stability tests, and dynamic modulus tests. Moreover, the performance of site mixtures was comparatively investigated with that of lab-made mixtures to further explore the site mixing effect on the mixture performance. The results showed that the recycled mixtures without basalt fiber presented unqualified cracking resistance even though proper mixture design was performed. The addition of basalt fibers could greatly enhance the rutting resistance, low-temperature cracking resistance, and stripping resistance of HIP recycled mixtures by 105.2%, 102.3%, and 46.9%, respectively. Moreover, the mixing method also had a significant impact on the properties of mixtures. The recycled mixtures produced by the site re-mixing method showed inferior performance compared to that of mixtures produced by the lab mixing method. Specifically, the dynamic stability, low temperature failure strain, and stripping point values reduced by 44.1%, 16.2%, and 11.7%, respectively, indicating that the site re-mixing process was not as effective as the lab mixing process due to the weaker blending and mixing procedures of the site equipment. The results could be beneficial for the utilization of basalt fiber in HIP recycling technology.

KEYWORDS

reclaimed asphalt pavement (RAP), hot in-place recycling (HIP), basalt fiber, site re-mixing recycled asphalt mixture, performance evaluation

1 Introduction

With vigorous upgrading of hot in-place recycling equipment and the demand for environmental protection in recent decades, hot in-place (HIP) recycling technology, which can re-use RAP materials, has gradually returned to a wide range of popularization and application (Banting and Yifu, 2021a). HIP recycling technology, which mainly treats cracks, potholes, rutting, and other minor diseases on the surface layer of pavement has significant

benefits, with fewer procedures and higher efficacy, a high utilization rate of RAP, and low impact on traffic (Pan et al., 2021). Meanwhile, it is also well known for the benefits of energy conservation and emission reduction (Di et al., 2021). It has been reported that using this technology can reduce maintenance costs by more than 5% and greenhouse gas emissions by more than 16% (Banting et al., 2021b) when compared with milling-and-filling technology.

However, HIP recycling technology also presents some limitations. The quality of the recycled mixtures is difficult to be accurately controlled due to uncertain variability, resulting in a decrease in the recycling effect of asphalt pavements. Moreover, hot in-place recycling also shows climate dependent properties and is not suitable for construction in cold climates (Yue et al., 2020). When this technology is used in alpine areas, the compaction of the mixture appeared to be insufficient, caused by the site temperature difference coupled with high RAP dosing (Ma et al., 2021). In addition, there is the fact that the high RAP incorporation of this technology challenges the performance of recycled asphalt pavements. Studies have shown that too high dosage of RAP will result in inferior road performance of the mixtures after a certain period of service time (Bouraima et al., 2019; Yang et al., 2019; Pawel et al., 2022), which can be attributed to the insufficient homogeneity of the RAP and the new added mixtures. The issue of HIP recycled asphalt mixture performance enhancement still needs to be addressed.

Basalt fibers are currently used in asphalt mixtures and confer a satisfactory enhancement effect to the mixture properties, due to their high strength and excellent toughness, along with environmental protection and pollution-free characteristics (Cheng et al., 2023). In the Jiangsu Province of China, more than 1,500 km of basalt fiber–strengthened asphalt pavements have been constructed over the past several years. Furthermore, studies have focused on the effect of basalt fibers on the pavement properties of asphalt mixtures, and the results have generally proved that basalt fibers can significantly enhance the resistance to high-temperature deformations, low-temperature cracking, freezing and thawing resistance, and especially fatigue resistance, thus enhancing the durability of the pavements and prolonging their service life (Lou et al., 2021a; Lou et al., 2021b; Keke et al., 2021). Guo et al. used asymmetric semicircular bending tests to investigate the Type I and Type II cracking modes of basalt fiber–reinforced asphalt mixtures at low and intermedium temperatures. The results showed that basalt fibers have the best reinforcing effect on the mixture fracture resistance (Qinglin et al., 2021). Wu's research showed that basalt fibers can substantially improve the high and low temperature cracking resistance of a central plant hot recycling mixture (Xiang et al., 2022). Thus, this study aims to introduce basalt fibers into HIP recycling asphalt mixtures, with the expectation of enhancing the corresponding road performance and mechanical properties.

However, the recycling process of HIP is also one of the key factors affecting the recycled mixture's performance, including construction temperature, heating method, on-site mixing, and type and dosage of additives (Yuquan et al., 2023). When basalt fibers are used in HIP recycling technology, the properties of the HIP recycled asphalt mixtures might not meet expectations due to limitations regarding mixing equipment and the uncertainty of on-site construction (Banting et al., 2021c). In this study, three types of basalt fiber–modified recycled mixtures were prepared using different mixing methods, namely, type A (site mixture), type B (plant and lab mixture), and type C (lab mixture). Specifically, type A simulates the site re-mixing of RAP and central plant preparation of new mixtures. Type B simulates the lab mixing of RAP and central plant preparation of new mixtures, while type C presents the lab mixing of RAP and lab preparation of new mixtures. Subsequently, the wheel tracking test, uniaxial penetration test, dynamic creep test, low-temperature beam bending test, semicircular bending test, water stability test, Hamburg rutting test, and dynamic modulus test were conducted to comparatively investigate the effects of site remixing and lab mixing methods on the performance of hot in-place recycled mixtures.

2 Raw materials and methodologies

2.1 Raw materials

2.1.1 Reclaimed asphalt pavement (RAP)

The RAP used for this study was obtained from the national main trunk line, named G233 Baoying section, in Jiangsu Province. The dense gradation with a nominal maximum particle size of 13.2 mm (namely, SUP-13) and petroleum asphalt with a grade of 70# were used for original application. The hot milling process, by which the pavement was heated before being milled, was utilized to obtain the RAP, so as to protect the original gradation of the pavement. Then, the old asphalt was extracted, and the mineral gradation was determined according to the specifications of (JTG, 2011) E20-T0722 and T0725. The properties of the extracted old asphalt and the mineral gradation of the RAP are summarized in Tables 1, 2.

It can be seen from Table 1 that, compared with the original new asphalt, the extracted old asphalt becomes stiffer, resulting in lower penetration, a higher softening point and viscosity, and a significantly lower ductility. It can be seen from Table 2 that the passing percentages at sieve sizes of 1.18 and 0.6 mm are located in the restricted zone, indicating that the mineral gradation of RAP contains more fine aggregates since some coarse aggregates have been crushed. Therefore, the gradation of the RAP needs to be adjusted by adding new aggregates for the HIP recycling application.

2.1.2 Rejuvenating agent

The rejuvenating agent RA-102, which is produced by Subote New Materials Co., was used in this study. The technical indexes of this agent all meet the Requirements in the specification of JTG/T 5521-2019. Specifically, the viscosity at 90°C is 4,000 cp. Flashpoint is 248°C. Saturated fraction and aromatic content is 25.6%, and 53%, respectively.

2.1.3 New aggregates and new asphalt

Basaltic coarse and fine aggregates were selected as the new aggregates. Moreover, limestone mineral powder was chosen as the mineral filler. The properties of all the aggregates and fillers were tested based on the Test Procedure for Aggregates in Highway Engineering (JTG E42), and the test results were all in accordance with the corresponding requirements in the test specification.

TABLE 1 Property results of extracted old asphalt.

Property	Old asphalt	Original new asphalt	Test method JTG E20
Penetration (25°C)/0.1 mm	45.5	68.2	T0604
Softening point/°C	58	48.5	T0606
Ductility/mm	8.7 (15°C)	41.3 (5°C)	T0605
Viscosity(135°C)/Pa·s	1.28	0.87	T0613

TABLE 2 Mineral gradation of RAP.

Sieve size/mm	16.0	13.2	9.5	4.75	2.36	1.18	0.6	0.3	0.15	0.075
Passing percentage/%	100.0	95.8	81.3	47.0	37.9	27.1	19.5	14.8	12.1	9.2
Control point/%	—	90–100	≤90	—	28–58	—	—	—	—	2–10
Restricted zone/%	—	—	—	—	39.1	25.6–31.6	19.1–25.1	15.5	—	—

TABLE 3 Technical index of basalt fiber.

Index	Result	Test method
Diameter/μm	17.5	GB/T 7690.5
Length range/mm	3–9 mixed length	JT/T 776.1
Fracture strength/MPa	2,430	GB/T 20310
Elongation at break/%	3.0	GB/T 20310
Modulus of elasticity/GPa	84.5	GB/T 20310
Heat resistance, retained fracture strength/%	94.8	JT/T 776.1
(Fe2O3+FeO) content/%	9.68	GB/T 1549
Acidity factor	6.1	GB/T 1549

The SBS-modified asphalt with a PG grade of 76-22, which with the penetration value of 71 (0.1mm), softening point of 80°C, separation of 1.4°C, and elastic recovery of 76%, was chosen in this study.

2.1.4 Basalt fiber for hot in-place recycling

The basalt fiber chosen for this study was from Jiangsu Tianlong Basalt Continuous Fiber Co., Ltd. The technical properties are shown in Table 3.

2.2 Mixture design

2.2.1 Gradation

As mentioned above, the gradation of the RAP needed to be adjusted by adding new aggregates to qualify it. Based on the design document of the G233 maintenance project, it was determined that the gradation should be composed of 70% RAP and 30% new materials. The final synthetic gradation is shown in Figure 1.

In addition, 0.2% basalt fibers were added to promote the performance of the hot in-place mix. During the site application process, the basalt fibers were added using the following procedures: all the basalt fibers were added in the central plant to make a new mixture (as shown in Figure 2) and then the new mixture with fibers is transported to the site and mixed with the RAP on site. The optimum oil/aggregate ratio and related indexes of the recycled asphalt mixtures are shown in Table 4.

2.2.2 Determination of rejuvenating agent dosage

The recycled asphalt samples were prepared by mixing the extracted old asphalt with rejuvenating agent. The dosages were set to be 2%, 3%, 4%, and 6% by weight of the extracted old asphalt. Then, the indexes of needle penetration, softening point, and viscosity were tested, and the results are listed in Table 5. It could be observed in Table 5 that when the dosage reaches 3%, the penetration value exceeded 60 (0.1 mm) and the softening point and viscosity values were all close to those of the original 70# asphalt. Since excessive rejuvenating agent would affect the high temperature performance of recycled asphalt mixtures, a rejuvenating agent dosage of 3% was chosen for the mixtures.

2.2.3 Sample fabrication

According to the construction procedures of HIP recycling technology, the necessary materials were retrieved from different locations, as shown in Figure 3. The RAP materials, which have been heated and milled into a loose state, were retrieved at location ONE. The new asphalt mixtures, which were produced at the central plant and modified with basalt fibers, were retrieved from location TWO. Moreover, after the site mixing process for the RAP and new materials, the recycled asphalt mixtures were retrieved at the discharge outlet of the site mixing equipment, i.e., location THREE. In addition, a continuous drum mixer was used for site mixing with the mixing time of 40 s. Comparatively, a batch mixer was utilized for lab mixing with the mixing time of 90 s.

Then, three types of mixture samples were fabricated using different methods. Samples of type A were prepared by using the recycled asphalt mixtures retrieved from location THREE; it should be emphasized that no further lab mixing process was applied to these mixtures. Samples of type B were prepared by mixing the RAP

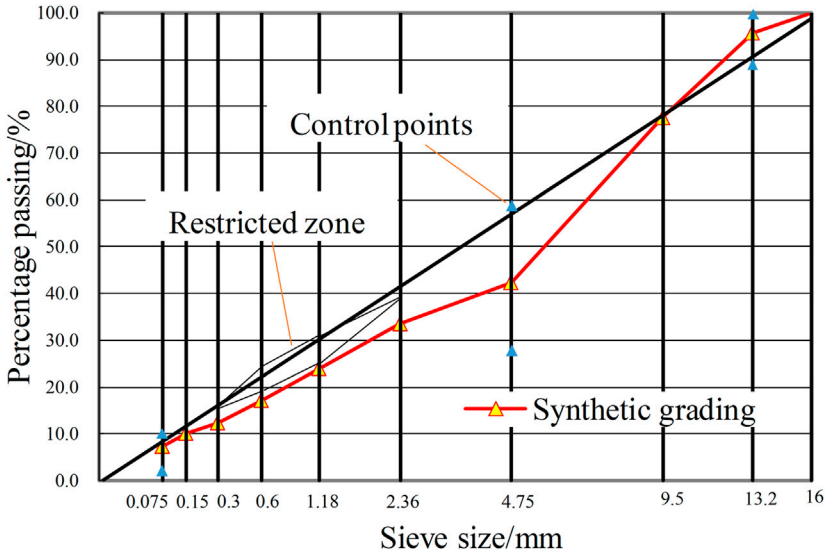

FIGURE 1
Synthetic gradation curve of SUP-13.

FIGURE 2
Fiber dispersion in the central plant new mixtures.

materials from location ONE and the new materials from location TWO in the lab. Samples of type C were fabricated by mixing the RAP materials from location ONE and lab-made new materials in the lab. The only difference between type B and type C mixtures was the source of the new materials. By comparing the type B and type C mixtures, the performance of the new mixtures from the central plant can be evaluated. The mixing methods are summarized in Table 6. In addition, a type N mixture with no fiber was also prepared by lab mixing as a control group.

2.3 Test methods

2.3.1 High temperature stability tests

(1) Rutting test

The rutting test was conducted according to the specifications of JTG E20-2011. This test was usually conducted for 1 h at 60°C by recording the rutting depth at 45 and 60 min; the dynamic stability can be calculated using Eq. 1. The test required an asphalt mixture slab with dimensions of 50 mm × 300 mm × 300 mm, which was maintained at 60°C for at least 5 h and then subjected to the rutting test, with three duplicates per group.

$$DS = \frac{N(t_2 - t_1)}{d_2 - d_1} \times C_1 \times C_2 \quad (1)$$

TABLE 4 Optimum oil/aggregate ratio and related indexes of recycled asphalt mixtures.

Property	No-fiber	0.2% basalt fiber	Requirement
Optimum oil/aggregate ratio/%	4.6	4.7	—
Marshall stability/kN	12.2	15.7	≥8.0
Flow value/mm	3.85	3.13	2–5
Air voids/%	4.8	4.9	4.0–6.0
Voids filled with asphalt (VFA)/%	66.4	66.7	65–75
Voids in mineral aggregate (VMA)/%	14.3	14.6	≥14.0

TABLE 5 Properties of recycled asphalt with different rejuvenating agent dosages.

Property	Regenerating agent dosage					Original 70# asphalt	Test method JTG E20
	0	2	3	4	6		
Penetration (0.1 mm, 25°C)	45.5	53.2	61.5	64.2	69.3	68.2	T0604
Softening point (°C)	58	53.0	52.1	50.3	49.6	48.5	T0606
Rotational viscosity (Pa·s)	1.28	0.99	0.89	0.82	0.75	0.87	T0613

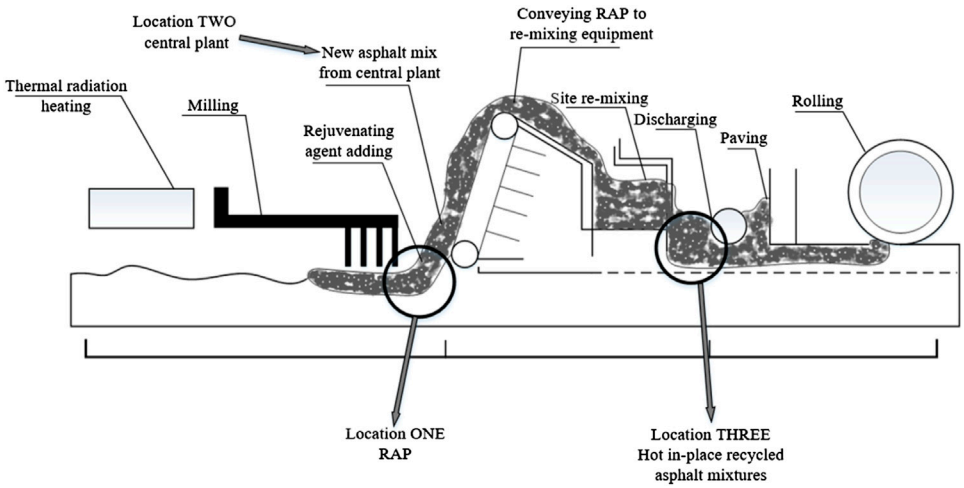

FIGURE 3
Illustration of material retrieval locations.

TABLE 6 Mixing methods for different types of mixtures.

Mixture type	New mixture preparation	RAP preparation	Mixing method
N (without fiber)	Lab fabrication without fiber	Lab heated	Lab mixing
A (site mixture)	Central plant with fiber	Site heated	Site re-mixing
B (plant and lab mixture)	Central plant with fiber	Lab heated	Lab mixing
C (lab mixture)	Lab fabrication with fiber	Lab heated	Lab mixing

where DS is the dynamic stability (times/mm), t_1 and t_2 are the test timings (min), d_1 and d_2 are the rutting depths at t_1 and t_2 timings (mm), N is the wheel speed, which is 42 times/min, and C_1 and C_2 are the test machine or specimen correction factors, which equal 1.0.

(2) Uniaxial penetration test

The uniaxial penetration test was carried out based on the specifications of JTG D50-2017 to evaluate the high temperature shear strength of the mix by calculating the penetration strength according to Eqs 2, 3. The test loading rate was 1 mm/min and the test temperature was 60°C, with five duplicates per group.

$$R_\tau = f_\tau \sigma_p \tag{2}$$

$$\sigma_p = \frac{P}{A} \tag{3}$$

where $R\tau$ is the revised penetration strength (MPa), σ_p is the penetration strength (MPa), P is the ultimate load when the sample fails (N), A is the indenter cross-sectional area (mm^2), and f_τ is the penetration stress factor, which is 0.35.

(3) Dynamic creep test

The dynamic creep test was performed by repeated axial loading using a cyclic load directly above the specimen, which was identical to that of the dynamic modulus test, with a test temperature of 60°C, based on the specifications of JTG E20-2011. Different loading levels of 0.7, 0.78, and 0.87 MPa were chosen to simulate a heavy-duty load

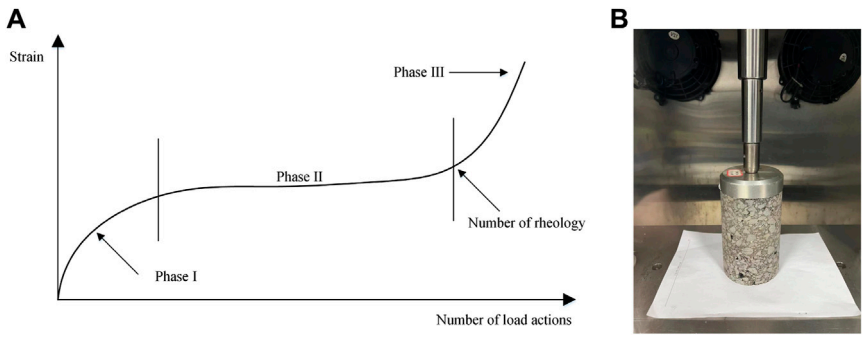

FIGURE 4
Illustration of the dynamic creep test. **(A)** Typical curve. **(B)** Test procedure.

and a standard load. The test was ended when the specimen produces 100,000 micro-strains or suffers10,000 loading cycles. The dynamic creep behavior tended to evolve along three stages with an increase in the number of load actions. An illustration of the dynamic creep test is shown in Figure 4.

The first stage was the creep migration stage, in which the strain rises sharply until a certain point. The second stage was the creep stabilization stage, in which the strain maintains a linear growth trend for a long period. The third stage was the creep damage stage, in which the strain increases sharply until the failure (or end) point. A mathematical model of accumulated strain versus load cycle can be established for each stage, as shown in Eqs 4–6.

$$\text{Phase I (pressure dense phase)}.\ \varepsilon_P = aN^b, N < N_{\text{ps}} \tag{4}$$

$$\text{Phase II (creep stabilization)}.\ \varepsilon_P = \varepsilon_{PS} + c\,(N - N_{PS}), N_{PS} \le N \le N_{ST} \tag{5}$$

$$\text{Phase III (creep damage)}.\ \varepsilon_P = \varepsilon_{ST} + d\left(e^{f\,(N-N_{ST})}-1\right), N > N_{ST} \tag{6}$$

where ε_P is the accumulative micro-strain, *a, b, c,* and *d* are the fitting coefficients, N is the loading times, N_{PS} is the first and second stage critical repeated loading number, N_{ST} is the second and third stage critical repeated loading number, and ε_{PS} and ε_{ST} are the starting and ending cumulative micro-strain at phase II, respectively.

The slope of the linear growth graph in phase II is regarded as the creep rate, while the stage cut-off point of the second and third stages is considered as the flow number *Fn*.

2.3.2 Cracking resistance tests

(1) Low temperature bending beam test

The low temperature bending beam test was used to analyze the low temperature cracking resistance of the recycled asphalt mix, according to the specifications of JTG E20-2011. Prismatic beam samples with dimensions of 250 mm × 30 mm × 35 mm were prepared. The test was conducted at a temperature of −10°C and a loading rate of 50 mm/min, with four duplicates per group. The bending tensile strength (R_B), maximum failure strain (ε_B), and stiffness modulus (S_B) were calculated according to Eqs 7–9. The test procedure is shown in Figure 5.

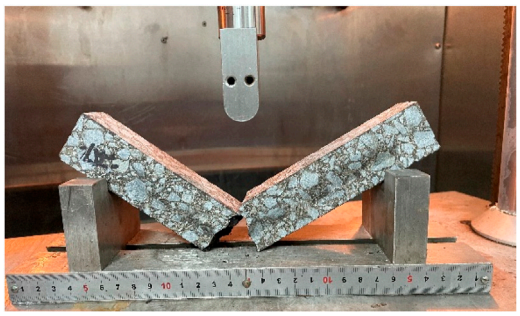

FIGURE 5
Illustration of low-temperature bending beam test.

$$R_B = \frac{3 \times L \times P_B}{2 \times b \times h^2} \tag{7}$$

$$\varepsilon_B = \frac{6 \times h \times d}{L^2} \tag{8}$$

$$S_B = \frac{R_B}{\varepsilon_B} \tag{9}$$

where b is the width of the specimen (mm), h is the height of the specimen (mm), L is the length of the specimen (mm), P_B is the maximum load (N), and d is the span deflection when the specimen fails (mm).

(2) Semi-circular bending test

The semi-circular bending (SCB) test was used according to the (AASHTO, 2016) TP 124–16 standard test method to assess the intermedium anti-cracking capability of the asphalt mixtures. Load and displacement curves were recorded during the SCB test, and the area enveloped by the curve was the fracture work generated during the cracking process. The ratio of the fracture work to the fracture area is called the fracture energy, as expressed by Eqs 10–12. A higher fracture energy value represents better anti-cracking performance. Four duplicates were used for one group.

$$G_f = \frac{W_f}{A_{lig}} \times 10^6 \tag{10}$$

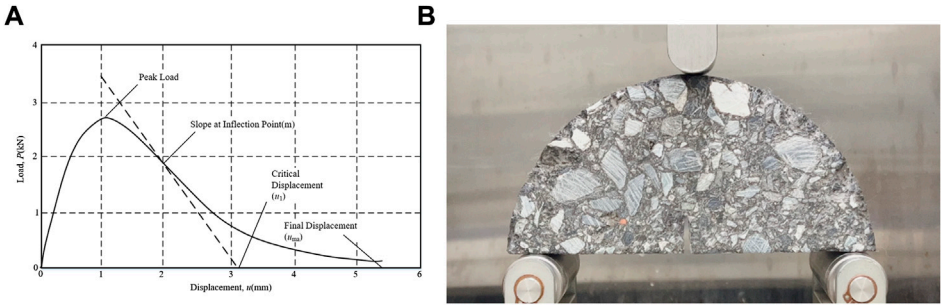

FIGURE 6
Illustration of semi-circular bending test. **(A)** Load (P) vs. displacement (u) curve. **(B)** Test procedure.

$$W_f = \int P du \tag{11}$$

$$A_{lig} = (r - a)t \tag{12}$$

where G_f is the fracture energy (J/m^2), W_f is the fracture work (J), A_{lig} is the fracture area (mm^2), *r-a* is the length of the fracture zone, and *t* is the thickness of the specimen (mm).

The flexibility index *FI* was proposed to characterize the crack propagation rate, as shown in Figure 6A. The *FI* index can be expressed by Eq. 13. The test procedure is shown in Figure 6B.

$$FI = \frac{G_f}{|m|} \times A \tag{13}$$

where *FI* is the flexibility index, $|m|$ is the absolute value of the post-peak slope (kN/mm), and *A* is the unit conversion coefficient, which is 0.01.

2.3.3 Water stability tests

(1) Immersion Marshall test

The water stability of the asphalt mixture was tested using the immersion Marshall test in accordance with T0709-2011 in JTG E20-2011. According to Eq. 14, the residual stability of the specimen immersed in water was calculated, and four duplicates were used for one group.

$$MS_0 = \frac{MS_1}{MS} \times 100 \tag{14}$$

where MS_0 is the residual stability (%), *MS* is the Marshall stability (kN), and MS_1 is the stability after 48 h in a hot water bath (kN).

(2) Freeze-thaw splitting test

The freeze-thaw splitting test was carried out in accordance with JTG E20-2011"Test Procedure for Asphalt and Asphalt Mixtures for Highway Projects" (T0729-2000), with four duplicates per group. The test strength ratio is given by Eq. 15.

$$TSR = \frac{\bar{R}_{T2}}{\bar{R}_{T1}} \times 100 \tag{15}$$

where *TSR* is the freeze-thaw splitting test strength ratio (%), $\bar{R}_{T2}$ is the average value of the splitting tensile strength of the group of specimens after the freeze-thaw cycles (MPa), and $\bar{R}_{T1}$ is the average splitting tensile strength of the first group of specimens without freeze-thaw cycles (MPa).

(3) Hamburg rutting test

The Hamburg rutting test was carried out according to (AASHTO, 2014) T324, and can be used to comprehensively evaluate the water stability and high temperature performance of the mix. The test was run under a wheel pressure of 0.7 MPa and at a water bath temperature of 50°C, with three duplicates in each group. The termination conditions for each group of specimens in the test were when the wheel tracking number reached 20,000 times or the rutting depth reached 20 mm. As shown in Figure 7, a typical Hamburg rutting curve can be divided into three stages in terms of development trend: initial compaction stage, middle creep stage, and eventual stripping stage. The slope of the fitted straight line in the mid creep stage was used as the creep rate. The slope of the fitted straight line in the eventual stripping stage was used as the stripping slope. The stripping point (SIP) was defined by the inflection point of deformation between the creep phase and stripping phase. The creep rate and rutting depth were the two indicators used to evaluate the rutting resistance. The greater the creep rate and rutting depth, the worse the rutting resistance. The stripping point is often used to evaluate the resistance to water damage, where a smaller stripping point value indicates poorer resistance to water damage.

2.3.4 Dynamic modulus test

The dynamic modulus test was conducted according to JTG E20-2011. Cylindrical specimens with dimensions of 100 mm in diameter and 150 mm in height were tested, as shown in Figure 8. The temperature was set at five levels: −10°C, 5°C, 20°C, 35°C, and 50°C. The load frequency was set at six levels: 0.1, 0.5, 1, 5, 10, and 25 Hz. The test procedure is shown in Figure 8. Three duplicates were used in each group.

3 Results and discussion

3.1 High temperature stability

(1) Results of the rutting test

The dynamic stability (DS) results from the rutting tests are illustrated in Figure 9. It can be seen from Figure 9 that, compared

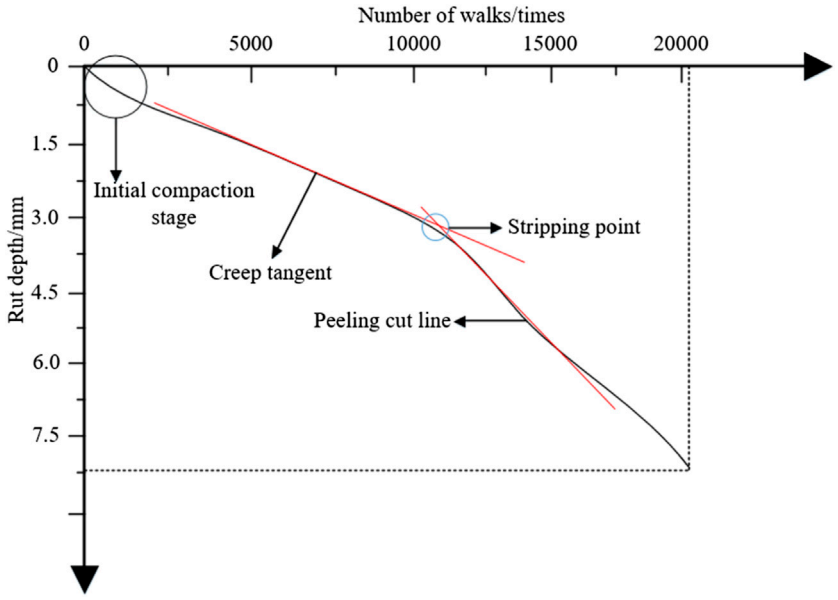

FIGURE 7
Typical Hamburg rutting test curves.

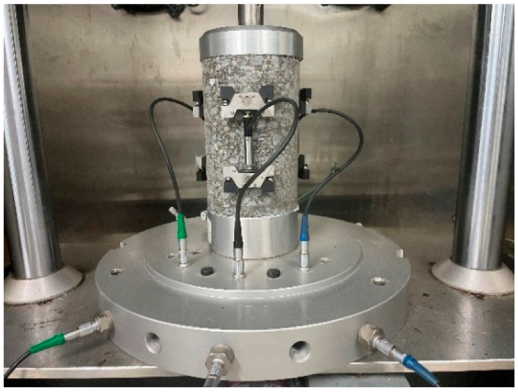

FIGURE 8
Dynamic modulus test procedure.

with the type N mixture without basalt fiber, the recycled asphalt mixtures of type A, B, and C all presented much higher dynamic stability values, which increased by 14.6%, 88.1%, and 105.2%, respectively. This indicates that basalt fiber can strengthen the anti-rutting property of the HIP mixture to a great degree, despite the mixing method.

Moreover, the mixing method also impacts the rutting resistance. The dynamic stability value of the type A mixture decreased from 7,789 passes/mm to 4,402 passes/mm, i.e., by 44.1%, compared to the type C mixture, although the values all met the minimum limitation of ≥3,000 passes/mm specified JTG E20-2011. These findings reflect that the recycled mixtures from the HIP re-mixing process show inferior rutting resistance to the lab mixing mixtures, even though the same raw materials were used. This might be attributed to the non-uniformity of the mixtures caused by site re-mixing (Yang et al., 2019).

In addition, minor differences in the DS values can be found between type B and type C mixtures; lower than 10%. Since the source of the new materials is the only difference between type B and type C mixtures, in which the new materials were produced from the central plant and lab-made, respectively. This minor difference infers that adding basalt fiber in the central plant to produce new mixtures can provide a comparative effect to the lab mixing method.

In general, when lab mixing mixtures are prepared to access the anti-rutting capability of the HIP mixture, a higher design DS value might be required, considering the uncertainty of HIP recycling technology.

(2) Results of the uniaxial penetration test

The results from the uniaxial penetration tests are illustrated in Figure 10. It can be noted from Figure 10 that the penetration strength (PS) values of different mixtures presented a similar trend to the DS results. Compared with the type N mixture without basalt fiber, the PS values of the recycled asphalt mixtures of type A, B, and C increased by over 24%. In terms of the effect of the mixing method, the PS values of the type A mixture similarly reduced by 15.7% compared to the type C mixture. As for the type B and type C mixtures, the PS values were almost equal.

In summary, recycled mixtures fabricated using the site re-mixing method show weaker shear resistance than lab mixing mixtures. However, adding basalt fiber can also strengthen the high temperature shear resistance to some extent. This can be attributed to the three-dimensional network formed by basalt fiber in the mixtures, which can resist the shear dislocation of aggregates at high temperatures (Guan et al., 2019).

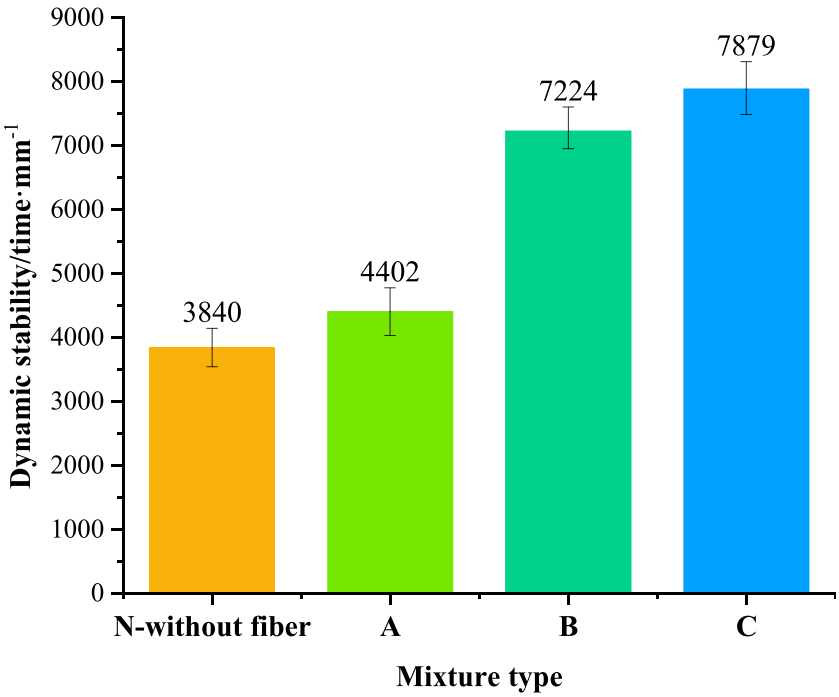

FIGURE 9
Rutting test results for specimens fabricated using different mixing methods.

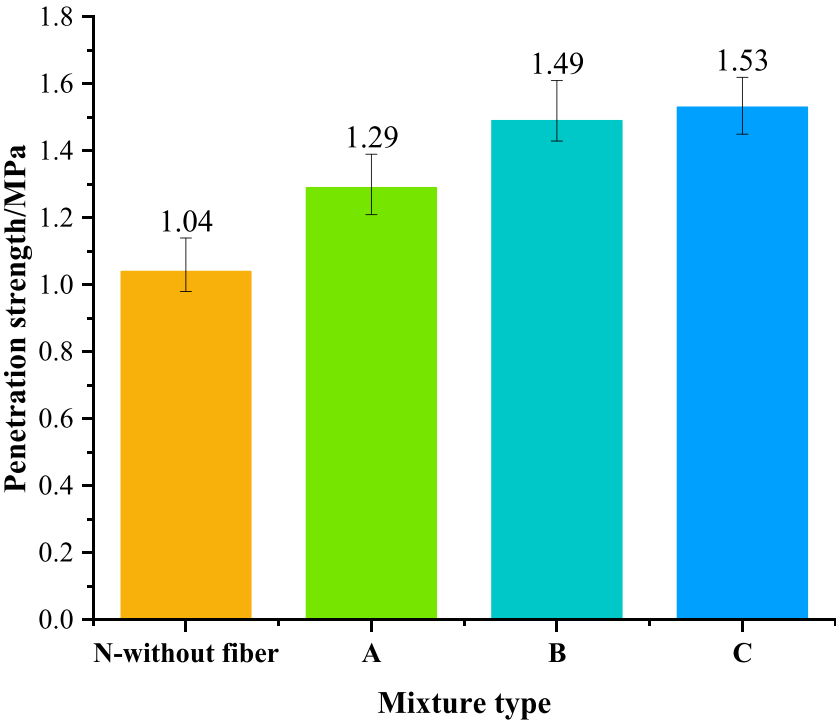

FIGURE 10
Uniaxial penetration test results for specimens fabricated using different mixing methods.

10.3389/fmats.2023.1332168

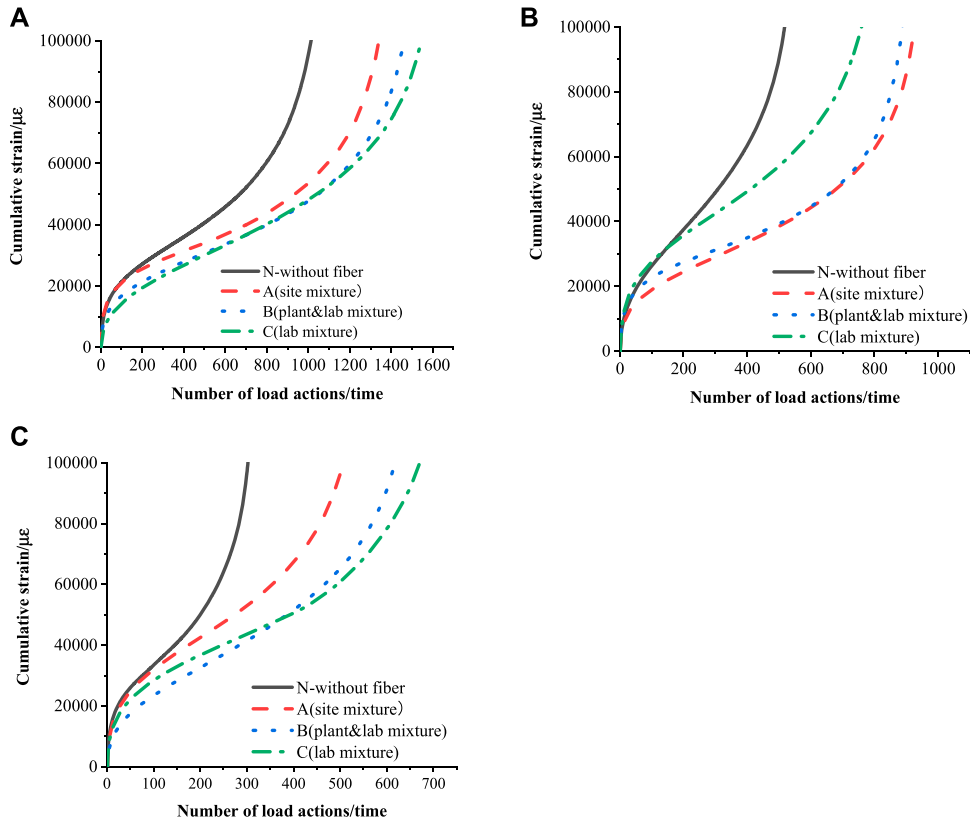

FIGURE 11
Test curves from dynamic creep test. **(A)** 0.7 MPa, **(B)** 0.78 MPa, and **(C)** 0.87 MPa.

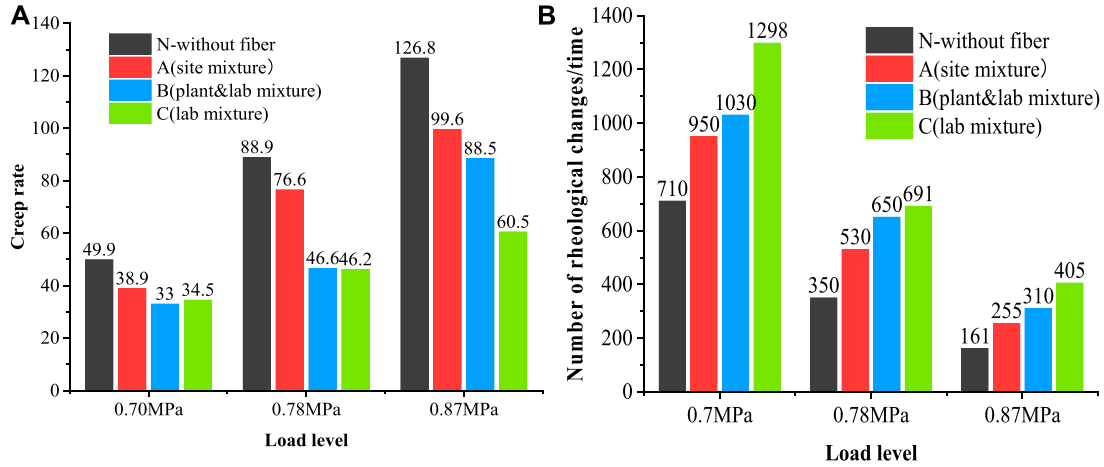

FIGURE 12
Test results of Dynamic creep test results. **(A)** Creep rate variation, **(B)** Rheological number variation.

(3) Results of the dynamic creep test

The curves for accumulative strain and number of load actions for the different mixtures are illustrated in Figure 11. The creep rate and flow number values were calculated, and the results are shown in Figure 12. It can be observed from Figure 12A that, compared to the type N mixture without fiber, the creep rate values of the type C mixture decreased by 30.8%, 48.0%, and 52.3% under 0.7, 0.78, and 0.87 MPa, respectively. In terms of flow number, as shown in Figure 12B, the values of the type C mixture increased by 82.8%, 97.4%, and 151.6%, respectively. These findings indicate that adding basalt fiber can decelerate the creep rate and enhance the permanent

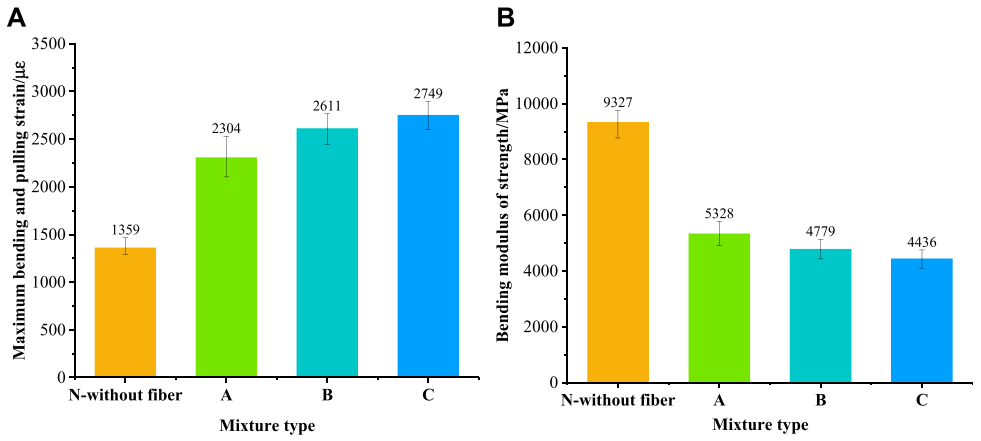

FIGURE 13
Results of the low-temperature bending beam test. **(A)** Results for the failure strain. **(B)** Results for the stiffness modulus.

deformation resistance of the recycled mix to a great extent. The enhancement impact becomes more prominent under higher load levels, which is consistent with Lei's research results (Lei et al., 2023).

Moreover, significant differences can also be observed in the creep rate and flow number values among mixtures fabricated using different mixing methods. Under the standard load level of 0.7 MPa, compared to the type C mixture produced by lab mixing, the creep rate values of the type A mixture increased by 12.8%, while the flow number values decreased by 26.8%. This indicates that the quality of site re-mixing during the HIP process can barely reach the same level as the lab mixing recycled mixture. In terms of type B and C mixtures, both the creep rates and flow number values were very similar, reflecting that, for the production of new mixtures with basalt fiber, the mixing process in the central plant shows equal effectiveness to mixing in the lab.

3.2 Crack resistance

(1) Results of the low temperature beam bending test

The maximum failure strain (ε_B) and stiffness modulus (S_B) obtained from the low temperature beam bending tests are presented in Figures 13A, B, respectively. In terms of the type N mixture without fiber, the failure strain value was as small as 1,359 με, which is much lower than the design limitation of ≥2,000 με, while the stiffness modulus (S_B) value reached as high as 9,728 MPa. These results are consistent with previous research findings that showed that HIP recycled mixtures present inferior low temperature cracking resistance (Yuan et al., 2021). This phenomenon might be attributed to the fact that aged asphalt makes the mixture stiffer, which is then prone to cracking (Xinghai et al., 2023).

When basalt fiber was added, the failure strain value of the type C mixture increased sharply by 102.3% compared to the type N mixture, while the stiffness modulus (S_B) value decreased from 9,728 to 4,436 MPa. This infers that basalt fiber can make the recycled mixture more flexible, subsequently leading to improved cracking resistance. The reason for this might be that the network formed by fibers can bear and dissipate stress in the mixture (Huan et al., 2023).

As for the different mixing methods, the failure strain value of the type C mixture was 19.3% higher than that of the type A mixture. Specifically, according to the (JTG, 2004) F40 specification, the low temperature cracking resistance of the type C mixture only reaches the "very cold zone" level ($\varepsilon_B \geq 2{,}300$ με), which is one level inferior to that of the type A mixture, which has a level of "extremely cold zone" ($\varepsilon_B \geq 2{,}600$ με). This indicates that the quality of the site-remixing recycled mixture needs to be improved. Moreover, the differences in failure strain values between the type B and C mixtures was within 6%, demonstrating the similar low-temperature performance of the two mixtures.

(2) Results of the semi-circular bending test

The fracture energy and *FI* values from the semi-circular bending tests are shown in Figure 14. It can be seen from Figure 14 that, compared with the type N mixture without fiber, the recycled asphalt mixtures of type C presented much higher G_f and *FI* values, which increased by 59.8% and 99.1%, respectively. This indicates that basalt fiber can not only enhance the fracture energy for crack initiation but can also decelerate the crack propagation rate.

In terms of the type A mixture, significant deterioration of the cracking resistance performance can be observed compared to the type C mixture. The G_f and *FI* values reduced by 37.7% and 33.6%, respectively. This indicates that the lab mixing method produces mixtures with superior cracking resistance to the site re-mixing method, which makes the mixture prone to crack initiation and propagation. Moreover, the G_f and *FI* values of the type B and C mixtures were very similar, indicating the comparable anti-cracking performance of the two.

3.3 Water stability

(1) Results of the immersion Marshall and freeze-thaw splitting tests

The residual stability (MS_0) and test strength ratio (*TSR*) values are shown in Figure 15. It can be observed from Figure 15 that all the

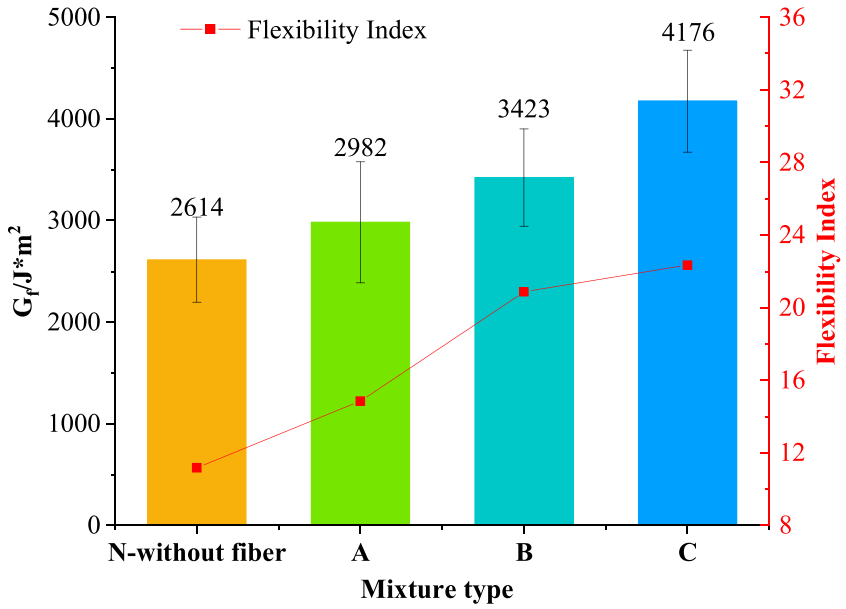

FIGURE 14
Results of semi-circular bending test.

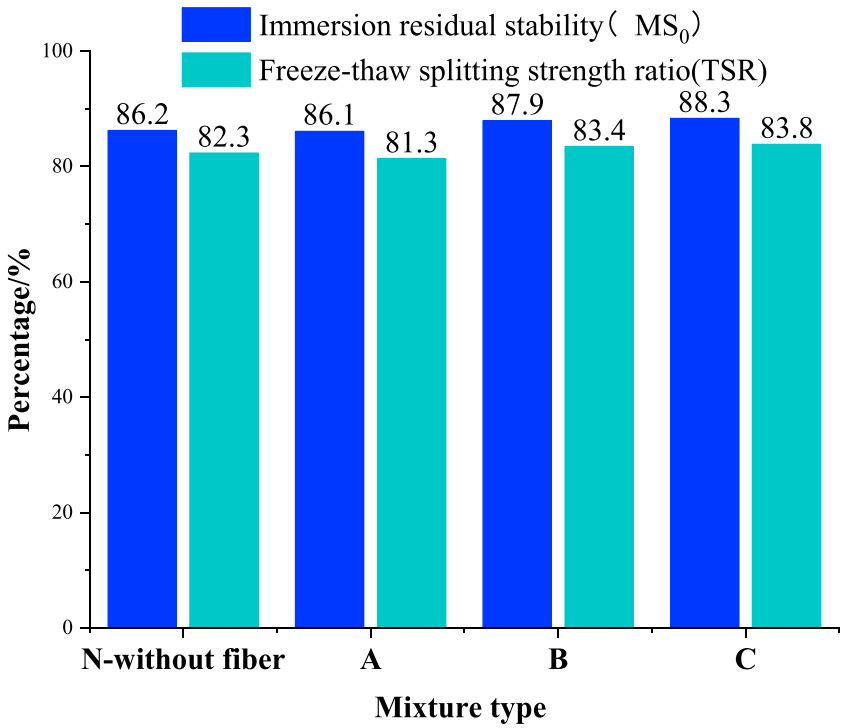

FIGURE 15
Results for MS_0 and *TSR* values.

MS_0 values were located in the range of 86.2%–88.3%, which all met the minimum limitation of ≥85% in the JTG E20-2011 specification. Moreover, all the TSR values were approximately 82%, meeting the requirement of ≥80% in the JTG E20-2011 specification. Furthermore, no obvious gap can be found for either the MS_0 or *TSR* values. It can be inferred from these two indicators that adding basalt fiber or using a different mixing method has no significant impact on the water stability of HIP recycled mixtures.

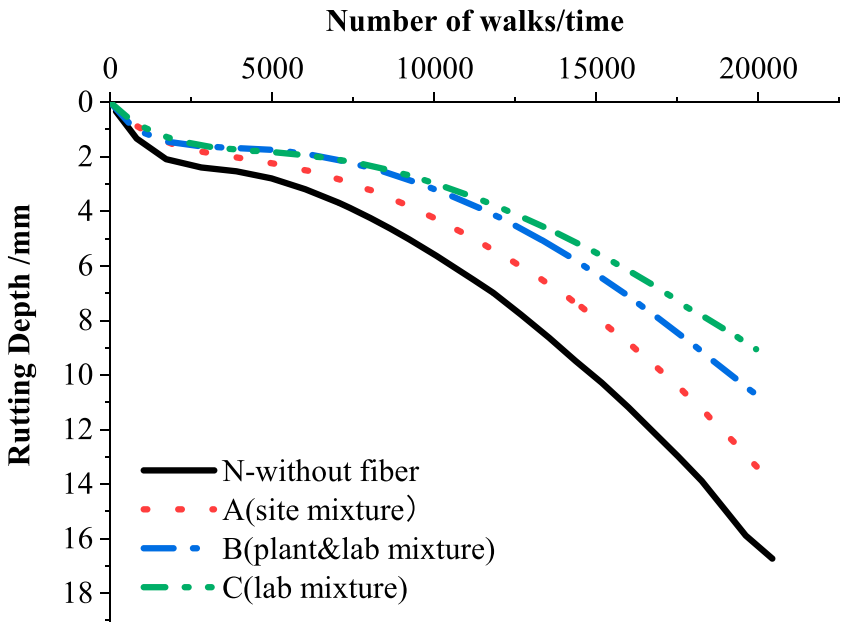

FIGURE 16
Curves from Hamburg rutting test.

TABLE 7 Calculated indicators from the Hamburg rutting test.

Pick-up molding method	Maximum rutting depth/mm	Creep rate/ mm·time^{-1}	Stripping slope/ mm·time^{-1}	Stripping point/ time
N(without fiber)	16.25	1.92×10^{-4}	6.83×10^{-4}	5,461
A (site mixture)	13.44	1.59×10^{-4}	5.49×10^{-4}	7,086
B (Plantandlab mixture)	11.04	1.29×10^{-4}	3.76×10^{-4}	7,831
C (lab mixture)	9.06	1.20×10^{-4}	3.28×10^{-4}	8,024

(2) Results of the Hamburg rutting test

The curves of the rutting depth, along with the walk number, are illustrated in Figure 16. The calculated creep rate and stripping point values are summarized in Table 7. It can be seen from Figure 16 that, unlike the results of the immersion Marshall and freeze-thaw splitting tests, significant differences can be observed from the rutting depth curves. All the mixtures presented the stripping stage, indicating that water damage occurs for the recycled mixtures. Specifically, analysis can be conducted based on the data in Table 7.

Compared with the type N mixture, the maximum rut depth of the type C mixture reduced sharply from 16.25 to 9.06 mm, while the creep rate decreasing by 37.5% and the stripping point improved by 46.9%. This infers that adding basalt fiber can effectively strengthen the rutting resistance and water stability under moisture and heat conditions.

In terms of the type A mixture, inferior performance could also be found from the Hamburg rutting test, presenting a higher maximum rut depth, larger creep rate, and lower stripping point compared to the type C mixture. In addition, comparable performance could be observed between the type B and C mixtures.

Overall, the results from the Hamburg rutting test could be used to distinguish the water stability of the HIP recycled mixture more effectively than the immersion Marshall and freeze-thaw splitting tests.

3.4 Dynamic viscoelastic properties

Master curves were established according to the results of the dynamic modulus test, as shown in Figure 17. A larger dynamic modulus value in the low frequency zone represents better permanent deformation resistance of the asphalt mixture. In contrast, a smaller dynamic modulus value in the high frequency zone indicates the superior flexibility and cracking resistance of the mixture (Liyan et al., 2022).

It can be seen from Figure 17 that, in the low frequency (high temperature) zone, the type N mixture without fiber displayed the lowest dynamic modulus, while the type C mixture presented the maximum value, followed by the type B and type A mixtures. This indicates that adding basalt fiber can increase the high-temperature performance of the HIP recycled mixture, which is consistent with the results from the high temperature stability

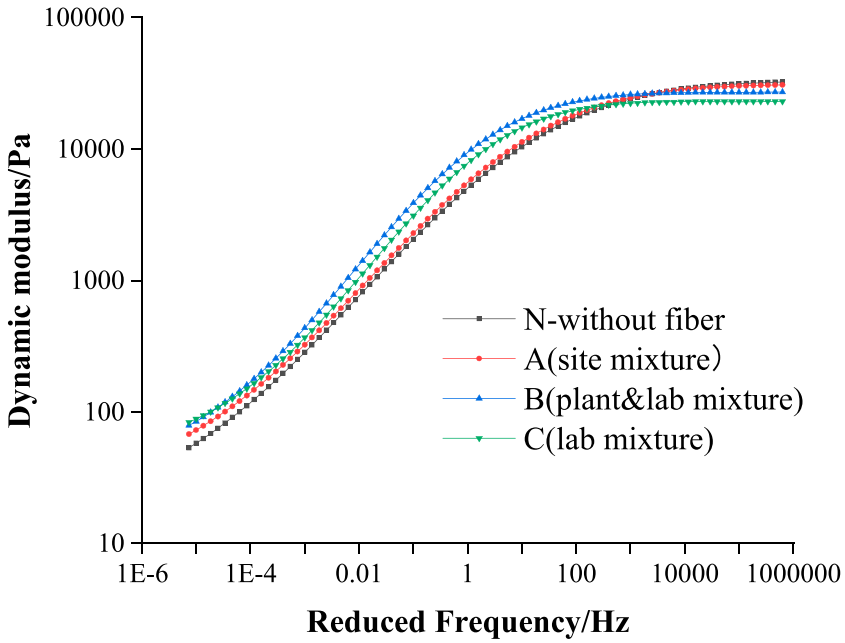

FIGURE 17
Master curve of the dynamic modulus of different mixtures.

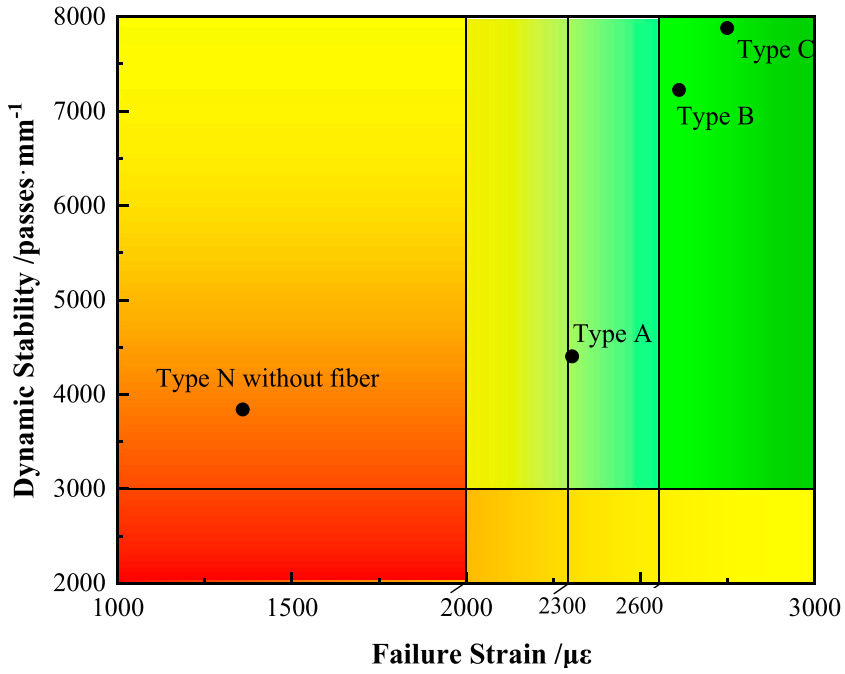

FIGURE 18
DS-FS performance-space chart.

tests in Section 3.1. Meanwhile, in the high frequency (low temperature) zone, the type C mixture presented the lowest dynamic modulus, while the type N mixture exhibited the maximum value, followed by the type A and type B mixtures. This indicates that the HIP recycled mixture without fiber possesses inferior cracking resistance, and that basalt fiber

improves the flexibility of the recycled mixtures at low temperature, improving their anti-cracking performance.

3.5 Comprehensive analysis

The so-called "DS-FS performance-space Chart" was developed, which was inspired by the "Hamburg-DC(T) Performance-Space Diagram" put forward by Buttlar et al. (2017). This chart can visually, synchronously, display the effect of basalt fiber and (or) the mixing method on the high and low temperature performance of the HIP recycled mixtures. This chart is plotted with dynamic stability (DS) values on the *y*-axis and failure strain (FS) on the *x*-axis, as presented in Figure 18.

According to the design requirement of the HIP recycling project, the DS value from the wheel tracking test is no less than 3,000 passes/mm. Meanwhile, based on the Chinese standard JTG F40, the FS values from the low temperature bending beam test are divided into three thresholds; specifically, mixtures with FS values of 2000–2,300 με, 2,300–2,600 με, and ≥2,600 με are suitable for the winter standard and heavy cold regions, the winter very cold region, and the winter extremely cold region, respectively.

It can be observed from Figure 18 that the DS values of the different mixtures all met the permanent deformation resistance requirement; however, the low-temperature cracking resistance of the type N mixture was far from qualified due to the high RAP content in the recycled mixture. These findings are consistent with previous results (Dong et al., 2020). When basalt fiber was added, both the rutting and cracking resistance presented a sharply increasing trend, as shown in the performance dot of the type C mixture, of which the FS value is located in the threshold of the winter extremely cold region. It improved three levels compared to the type N mixture. These findings prove that basalt fiber confers an excellent enhancement effect in hot in-place recycled mixtures compared to the fiber being used in fresh asphalt mixtures (Lou et al., 2021) or in central plant recycled mixtures (Davar et al., 2017).

Furthermore, both the DS and FS values of the type A mixture were much lower than those of the type C mixture. This indicates that the site re-mixing process is not as effective as the lab mixing process, leading to inferior performance of the site recycled mixtures compared to that of the lab mixing asphalt mixtures. Moreover, the mixing effect of the central plant is satisfactory since the overall performances of the type B and C mixtures are almost equal. Therefore, the main reason causing the performance difference between the type A and C mixtures can be attributed to the weaker blending and mixing procedures of the site equipment.

Furthermore, to enhance the properties of HIP recycle mixtures, innovative development of the site mixing process is essential, along with new additives such as basalt fibers.

4 Conclusion

Basalt fibers were introduced into hot in-place recycled asphalt mixtures to improve the pavement performance. The impact of the mixing method on the performance was also comparatively investigated. Based on the conditions used in this study, the following conclusions could be drawn:

(1) Based on the maintenance project of the G233 Baoying section in China, the dynamic stability and failure strain of the HIP recycled mixture reaches only 3,840 pass/mm and 1,359 με, respectively, presenting unqualified low temperature cracking resistance.
(2) Adding basalt fiber into HIP recycled mixtures can effectively improve the rutting resistance by over 105%, the cracking resistance by up to three low temperature threshold levels, and the stripping resistance by 46.9%, indicating that basalt fibers are effective in strengthening the mixture performance, even for HIP recycled mixtures.
(3) The Hamburg rutting test with a hot bath was far more effective than conventional water stability tests, such as the immersion Marshall and freeze-thaw splitting tests, in distinguishing the moisture damage resistance of recycled mixtures.
(4) The performance of recycled asphalt mixtures produced by the site re-mixing process was inferior to that of lab-made mixtures, which demonstrates that the effectiveness of the site re-mixing process needs to be improved to further improve the mixture performance.

This manuscript mainly focused on a comparative performance evaluation of site mixture versus lab mixture for HIP technology, from the perspective of lab experiments. However, knowledge of the effect of mixing process indexes such as mixing time, mixing power, mixing temperature, etc. on the performance is still lacking, which will be further investigated in subsequent research work.

Data availability statement

The original contributions presented in the study are included in the article/Supplementary Material, further inquiries can be directed to the corresponding author.

Author contributions

BL: Conceptualization, Formal Analysis, Methodology, Project administration, Visualization, Writing–original draft. YuZ: Data curation, Formal Analysis, Investigation, Methodology, Visualization, Writing–original draft. PX: Conceptualization, Funding acquisition, Project administration, Supervision, Writing–review and editing. YW: Formal Analysis, Methodology, Project administration, Writing–review and editing. AK: Conceptualization, Funding acquisition, Project administration, Supervision, Writing–review and editing. YaoZ: Investigation, Methodology, Visualization, Writing–review and editing.

Funding

The author(s) declare financial support was received for the research, authorship, and/or publication of this article. This research

was funded by the National Natural Science Foundation of China, grant numbers 52178439 and 52108422 and the Postgraduate Research and Practice Innovation Program of Jiangsu Province (Yangzhou University) (SJCX22_1751). In addition, this research was funded by the Postgraduate education and teaching reform and practice project of Yangzhou University, grant number JGLX 2021_010.

Acknowledgments

The authors want to thank the Yangzhou University Test Center for their assistance in providing some of the test instruments and materials.

Conflict of interest

The authors declare that the research was conducted in the absence of any commercial or financial relationships that could be construed as a potential conflict of interest.

Publisher's note

All claims expressed in this article are solely those of the authors and do not necessarily represent those of their affiliated organizations, or those of the publisher, the editors and the reviewers. Any product that may be evaluated in this article, or claim that may be made by its manufacturer, is not guaranteed or endorsed by the publisher.

References

AASHTO. (2016). Determining the fracture potential of asphalt mixtures using semicircular bend geometry (SCB) at intermediate temperature: AASHTO TP124-16[S]. [2016-08].

AASHTO (2014). Hamburg wheel-track testing of compacted asphalt mixtures: AASHTO T 324-22[S]. [2014-02].

Banting, W. P. S., and Yifu, Z. (2021a). Adaptability and key concepts of the hot in-place recycling technology. *Woodhead Publ. Ser. Civ. Struct. Eng.*, 13–15. doi:10.1016/B978-0-12-822422-9.00002-3

Banting, W. P. S., and Yifu, Z. (2021b). Construction process of the hot in-place recycling technology. *Woodhead Publ. Ser. Civ. Struct. Eng.*, 117–133. doi:10.1016/B978-0-12-822422-9.00005-9

Banting, W. P. S., and Yifu, Z. (2021c). Requirements of equipment for the hot in-place recycling technology. *Woodhead Publ. Ser. Civ. Struct. Eng.*, 95–115. doi:10.1016/B978-0-12-822422-9.00004-7

Bouraima, M. B., Zhang, X. H., Rahman, A., and Qiu, Y. (2019). A comparative study on asphalt binder and mixture performance of two traffic lanes during hot in-place recycling (HIR) procedure. *Constr. Build. Mater.* 223, 33–43. doi:10.1016/j.conbuildmat.2019.06.201

Buttlar, W. G., Hill, B. C., Wang, H., and Mogawer, W. (2017). Performance space diagram for the evaluation of high- and low temperature asphalt mixture performance. *Road. Mater. Pavement.* 18, 336–358. doi:10.1080/14680629.2016.1267446

Cheng, S., Jianan, W., Shuang, S., Lv, D., Xu, L., and Zhang, S. (2023). Research on properties of basalt fiber-reinforced asphalt mastic. *Front. Mater.* 10. doi:10.3389/fmats.2023.1277634

Davar, A., Tanzadeh, J., and Fadaee, O. (2017). Experimental evaluation of the basalt fibers and diatomite powder compound on enhanced fatigue life and tensile strength of hot mix asphalt at low temperatures. *Constr. Build. Mater.* 153, 238–246. doi:10.1016/j.conbuildmat.2017.06.175

Di, W., Chiara, R., Babak, J., Cannone Falchetto, A., and Wistuba, M. P. (2021). Investigation on the effect of high amount of Re-recycled RAP with Warm mix asphalt (WMA) technology. *Constr. Build. Mater.* 312, 125395. doi:10.1016/j.conbuildmat.2021.125395

Dong, H., Yongli, Z., Yuanyuan, P., Liu, G., and Yang, T. (2020). Heating process monitoring and evaluation of hot in-place recycling of asphalt pavement using infrared thermal imaging. *Autom. Constr.* 111, 103055. doi:10.1016/j.autcon.2019.103055

Guan, B., Liu, J., Wu, J., Tian, H., Huang, T., et al. (2019) Investigation of the performance of the ecofriendly fiber-reinforced asphalt mixture as a sustainable pavement material. *Adv. Mater. Sci. Eng.* 2019, 1. 11. doi:10.1155/2019/6361032

Huan, X., Peng, W., Ning, L., Gao, J., Yang, L., Li, J., et al. (2023). Study on failure characteristics of basalt fiber reactive powder concrete under uniaxial loading. *Constr. Build. Mater.* 404, 133246. doi:10.1016/j.conbuildmat.2023.133246

JTG (2004). Technical specifications for construction of Highway asphalt pavements: JTG F40——2004[S]. [2004-09-04].

JTG (2011). Standard test methods of bitumen and bituminous mixtures for Highway engineering: JTG E20——2011[S]. [2011-09-13].

Keke, L., Peng, X., Bangwei, W., Kang, A., Wu, X., and Shen, Q. (2021). Effects of fiber length and content on the performance of ultra-thin wearing course modified by basalt fibers. *Constr. Build. Mater.* 313, 125439. doi:10.1016/j.conbuildmat.2021.125439

Lei, C., Wei, L., Minghui, C., Qian, Z., Chen, X., and Zheng, Z. (2023). Bleeding mechanism and mitigation technique of basalt fiber-reinforced asphalt mixture. *Case Stud. Constr. Mater.* 19, e02442. doi:10.1016/j.cscm.2023.e02442

Liyan, S., Yajie, W., Shuang, L., et al. (2022). Establishment of correlation model between compositions and dynamic viscoelastic properties of asphalt binder based on machine learning. *Constr. Build. Mater.* 364, 129902. doi:10.1016/j.conbuildmat.2022.129902

Lou, K., Xiao, P., Kang, A., Wu, Z., and Lu, P. (2021a). Performance evaluation and adaptability optimization of hot mix asphalt reinforced by mixed lengths basalt fibers. *Constr. Build. Mater.* 292, 123373. doi:10.1016/j.conbuildmat.2021.123373

Lou, K., Xiao, P., Tang, Q., Wu, Y., Wu, Z., and Pan, X. (2021b). Research on the micro-nano characteristic of basalt fiber and its impact on the performance of relevant asphalt mastic. *Constr. Build. Mater.* 318, 126048. doi:10.1016/j.conbuildmat.2021.126048

Ma, Y., Polaczyk, P., Hu, W., Zhang, M., and Huang, B. (2021). Quantifying the effective mobilized RAP content during hot in-place recycling techniques. *J. Clean. Prod.* 314, 127953. doi:10.1016/j.jclepro.2021.127953

Pan, Y., Han, D., Yang, T., Tang, D., Huang, Y., Tang, N., et al. (2021). Field observations and laboratory evaluations of asphalt pavement maintenance using hot in-place recycling. *Constr. Build. Mater.* 271, 121864. doi:10.1016/j.conbuildmat.2020.121864

Pawel, P., Yuetan, M., Rui, X., Jiang, X., Zhang, M., Liu, Y., et al. (2022). Influence of mobilized RAP content on the effective binder quality and performance of 100% hot in-place recycled asphalt mixtures. *Constr. Build. Mater.* 342, 127941. doi:10.1016/j.conbuildmat.2022.127941

Qinglin, G., Zhipeng, C., Pengfei, L., et al. (2021). Influence of basalt fiber on mode I and II fracture properties of asphalt mixture at medium and low temperatures. *Theor. Appl. Fract. Mech.* 112.

Xiang, M., Jiaqing, W., Yinyin, X., et al. (2022). Investigation on the effects of RAP proportions on the pavement performance of recycled asphalt mixtures. *Front. Mater.* 8 (4), 2809. doi:10.3389/fmats.2021.842809

Xinghai, P., Nasi, X., Chengdong, X., Zhou, X., Zhao, P., Ma, S., et al. (2023). Laboratory evaluation of different bio-oil recycled aged asphalts: conventional performances and microscopic characteristics. *J. Clean. Prod.* 428, 139442. doi:10.1016/j.jclepro.2023.139442

Yang, L., Hainian, W., Susan, L. T., Zhao, G., and You, Z. (2019). Effects of preheating conditions on performance and workability of hot in-place recycled asphalt mixtures. *Constr. Build. Mater.* 226, 288–298. doi:10.1016/j.conbuildmat.2019.07.277

Yuan, P., Dong, H., Tao, Y., et al. (2021). Field observations and laboratory evaluations of asphalt pavement maintenance using hot in-place recycling. *Constr. Build. Mater.* 271, 121864. doi:10.1016/j.conbuildmat.2020.121864

Yue, M., Pawel, P., Park, H., Jiang, X., Hu, W., and Huang, B. (2020). Performance evaluation of temperature effect on hot in-place recycling asphalt mixtures. *J. Clean. Prod.* 277, 124093. doi:10.1016/j.jclepro.2020.124093

Yuquan, Y., Jiangang, Y., Jie, G., et al. (2023). Strategy for improving the effect of hot in-place recycling of asphalt pavement. *Constr. Build. Mater.* 366, 130054. doi:10.1016/j.conbuildmat.2022.130054